

Large Multistream Data Analytics for Monitoring and Diagnostics in Manufacturing Systems

Samaneh Ebrahimi, Chitta Ranjan, and Kamran Paynabar

H. Milton Stewart School of Industrial and Systems Engineering,
Georgia Institute of Technology, Atlanta, GA, USA

Abstract

The high-dimensionality and volume of large scale multistream data has inhibited significant research progress in developing an *integrated* monitoring and diagnostics (M&D) approach. This data, also categorized as big data, is becoming common in manufacturing plants. In this paper, we propose an integrated M&D approach for large scale streaming data. We developed a novel monitoring method named Adaptive Principal Component monitoring (APC) which adaptively chooses PCs that are most likely to vary due to the change for early detection. Importantly, we integrate a novel diagnostic approach, Principal Component Signal Recovery (PCSR), to enable a streamlined SPC. This diagnostics approach draws inspiration from Compressed Sensing and uses Adaptive Lasso for identifying the sparse change in the process. We theoretically motivate our approaches and do a performance evaluation of our integrated M&D method through simulations and case studies.

1 Introduction

Recently, the problem of process monitoring and diagnosis using a large scale multi-stream data has become an active research area in statistical process control (SPC). The reason is twofold: first, sensing technologies have enabled fast measurement of a large number of process variables, resulting in large data streams, and, second, conventional multivariate methods such as Hotelling's T^2 , MEWMA, and MCUSUM (Sparks (1992); Wierda (1994)) are not scalable in terms of the computational time and the detection power.

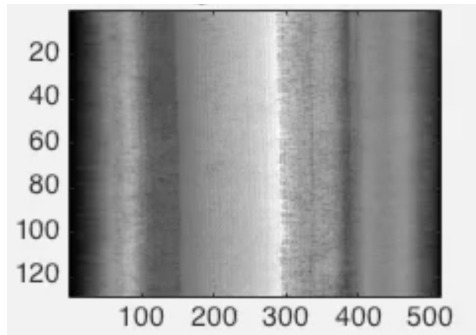


Figure 1: Surface image of steel bar in the rolling process

An example of large streams can be found in gas turbine systems used for power generation. In these systems, the performance of the confined combustion process is being monitored using hundreds of sensors measuring temperature, vibration, pressure, etc., in different chambers and segments of the turbine. Early detection of any changes in the system, followed by the diagnosis of the faulty variables is necessary to avoid imminent blowout that leads to relighting the combustor and costly shutdowns.

Another application of large streaming data is in image-based process monitoring in which each pixel of an image can be considered as a single data stream. For example, in a rolling process where a set of rollers are used to reduce the cross-section of a long steel bar by applying compressive forces, the quality of produced bars can be inspected by a vision system that is set up to take images of the bar surface at short time intervals. A sample of such an image is shown in Figure 1. In this image, each row contains 512 pixels, and each pixel can be considered as a variable resulting in an high-dimensional correlated data stream.

Despite its importance, existing SPC literature lacks a scalable integrated M&D approach using large data streams. In the following, we will discuss the existing work on *monitoring* and *diagnostics*, their shortcomings—especially their lack of integrability—, and motivate our approach.

Monitoring

Conventional multivariate monitoring charts are effective on small or moderate data streams. However, their performance deteriorates as the number of data streams increases. To address the high-dimensionality issue, more recent works have focused on employing variable selection

techniques to reduce the dimensionality by removing the variables that are less susceptible to the process change. Examples of the variable-selection-based method include Capizzi and Masarotto (2011); Wang and Jiang (2009); Zou and Qiu (2009). However, these methods are not scalable and generally require intensive computation as the dimension grows. Moreover, most of these methods are difficult to interpret for a process engineer.

There is a section of scalable multivariate monitoring methods that are developed based on the assumption that data streams are independent and the change is sparse (only a small subset of variables is affected by a process change). For example, Tartakovsky et al. (2006) assumed that exactly one variable changes at a time and proposed an approach based on the maximum of CUSUM statistics from each individual data stream. Mei (2010, 2011) developed robust monitoring scheme based on the sum of (the top- r) local CUSUM statistics assuming all variables are independent and measurable.

For the case that variables are not easily or efficiently measurable, Liu et al. (2015) presented TRAS (top- r based adaptive sampling), which is an adaptive sampling strategy that uses the sum of top r local CUSUM statistics for monitoring. The sparsity assumption is generally valid in practice as a change or fault often affects only a small subset of variables. However, although theoretically and computationally appealing, the independence assumption is typically unrealistic.

To address the dependency and high-dimensionality issues, Principal Component Analysis (PCA) has been widely used for monitoring multivariate data streams. PCA is a well-known projection technique that transforms dependent data to uncorrelated features known as Principal Component (PC) scores. Often, only a few PC scores that explain the most variation of original data are used for monitoring in a dimension reduction (Jackson and Mudholkar (1979); Li et al. (2014, 2000); Qahtan et al. (2015); Wise et al. (1990)). However, monitoring top PCs with the highest variance may not always be a right approach.

As an example, consider a bivariate normal distribution given in Figure 2, in which PC_1 represents the direction of the eigenvector with larger eigenvalue, and the red arrow indicates the direction of change in the mean of the distribution. As can be seen from the figure, the effect of the change on both PC-scores is the same. However, the fact that PC_1 constitutes

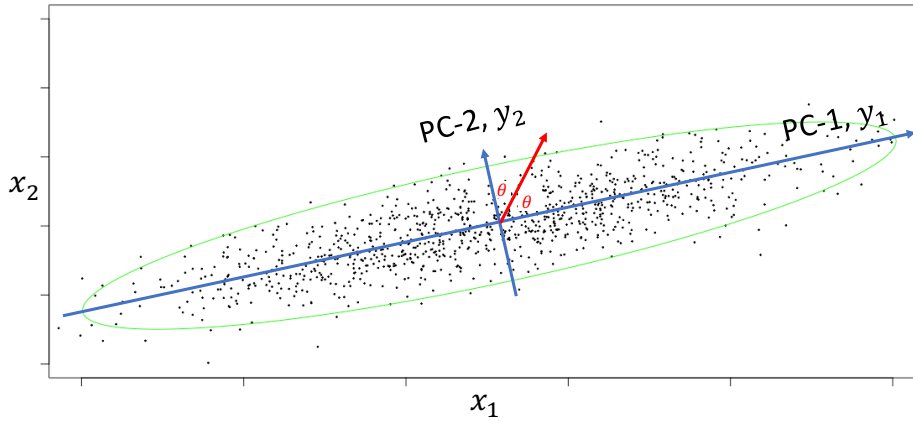


Figure 2: Example of a change having the same angle with both PCs

the most of the process variance makes it less sensitive to the change compared with PC2. In other words, small changes may be masked by the variation present in top PC scores, hence becoming undetectable.

Other PC selection criteria for process monitoring include the variance of reconstruction error (VRE) approach by Dunia and Joe Qin (1998), and the fault signal to noise ratio (SNR) by Yuan and Xiao-Chu (2009) and Tamura and Tsujita (2007). The VRE method selects a subset of PCs which minimizes fault reconstruction error, while the fault SNR method is based on fault detection sensitivity. The main disadvantage of these methods is that they require prior knowledge of the fault direction.

In this paper, we present an adaptive PC Selection (APC) approach based on hard-thresholding for selecting the set of PC scores that are most susceptible to an unknown change. Unlike the top-r-PCs, in our approach the number of features may vary at each sampling time. Also the PCs are adaptively selected based on the observed sample and its standardized distance from the in-control mean. Additionally, the proposed APC approach does not require any prior knowledge about a fault or change direction, which makes it more universally applicable.

Diagnostics

Another long-standing issue with PCA-based monitoring methods is the lack of diagnosability. This is because that the PC scores used as monitoring features are linear combinations of original measurements. Therefore, if a PC score initiates an out-of-control alarm, it is difficult to at-

tribute it to any specific process variable(s). Interpretation and decomposition of these additive statistics are often theoretically difficult and/or computationally expensive in high-dimensional data streams.

For diagnostics on a PC-based monitoring, one common approach is the use of contribution plots that specifies the contribution of each variable to the out of control statistic Alcalá and Qin (2009); Joe Qin (2003); Qin et al. (2001); Westerhuis et al. (2000). Contribution plots are popular because of their ease of implementation and their ability to work without any a priori knowledge. However, correct isolation with contribution plots is not guaranteed for multiple sensor faults Yue and Qin (2001).

To overcome this problem, hierarchical contribution plots was proposed MacGregor et al. (1994). However, it will perform poorly if the initial partitioning is not correct. Moreover, in the context of high-dimensional data, these methods become difficult to interpret and are also computationally expensive.

For the purpose of diagnosis in multivariate control charts with original measurements, Wang and Jiang (2009) and Zou and Qiu (2009) proposed variable selection techniques. Both methods optimize a penalized likelihood function for multivariate normal observations to identify the subset of altered variables. The \mathcal{L}_1 -penalized regression method of Zou and Qiu (2009) provides more computational advantages in implementation. Zou et al. (2011) combined Bayesian Information Criterion (BIC) with penalization techniques to assist the fault localization process and suggested an Adaptive Lasso-based diagnostic procedure. However, these methods assume that the change point is already known and focus only on diagnosis.

Additionally, they cannot easily be integrated with a PCA-based monitoring approach. To address these shortcomings, we propose a new diagnostics approach that seamlessly integrates with our proposed PCA-based monitoring method. The developed approach draws inspiration from Compressed Sensing and uses Adaptive Lasso to identify the shifted variables. In this paper, we focus on detecting mean shifts and we assume the shift is sparse. As mentioned earlier, this is a reasonable assumption because in real-world usually only a small number of variables change.

The major contributions in this paper are, a. countering the traditional view of top-PC

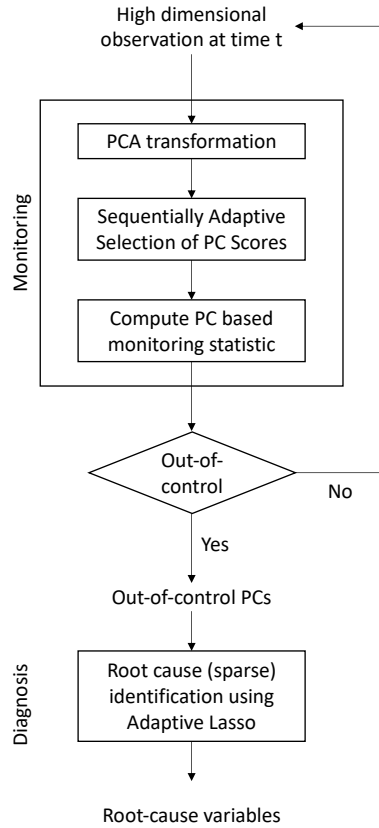


Figure 3: Methodology overview

scores as the best for process monitoring, and proposing an adaptive PC selection approach as an alternative; and b) proposing a new diagnostics approach that integrates with the proposed PCA-based monitoring framework. An overview of the proposed Monitoring and Diagnostics (M&D) approach is shown in Figure 3.

2 Integrated PCA-Based Monitoring and Diagnostics

2.1 Background

PCA is a linear transformation widely used for dimension reduction and generating uncorrelated features. Suppose a p -dimensional data stream denoted as $X = \{\mathbf{x}^{(t)} : \mathbf{x}^{(t)} \in \mathbb{R}^p; t = 1, 2, \dots\}$ is collected at sampling time t . Without loss of generality, assume the data streams

are centered (zero mean) with a covariance matrix Σ . By applying PCA, this set of correlated observations can be converted into a set of linearly uncorrelated variables known as *principal component scores*. The PC scores can be computed by $\mathbf{y} = A^T \mathbf{x}$, where $A \in \mathbb{R}^{p \times p}$ is the matrix of eigenvectors of Σ and $\mathbf{y} \in \mathbb{R}^p$ are the PCs. Also, it can be shown that $\text{var}(\mathbf{y}_j) = \lambda_j$ and $\text{cov}(\mathbf{y}_j, \mathbf{y}_k) = 0, \forall (j, k) \in \{1, \dots, p\}, j \neq k$.

For ease of interpretation, the eigenvectors in A are arranged such that their corresponding eigenvalues are in decreasing order, i.e. $\lambda_1 \geq \lambda_2 \geq \dots \geq \lambda_p$. This ordering will be further referred throughout the paper for developing our methodology. In this paper, we call the principal scores corresponding to higher and lower eigenvalues as top-PCs and bottom-PCs, respectively.

In most conventional PCA-based methods, top- k PCs are selected for monitoring because they contain more process information. This approach, however, may not always result in an appropriate set of monitoring variables. To illustrate this, we synthesized in-control samples of correlated data from a multivariate normal distribution with a dimension of 500 ($= p$) and $\boldsymbol{\mu} = \mathbf{0}, \boldsymbol{\sigma} = 0.1$ followed by out-of-control samples. In the out-of-control data, a random 10% set of variables are shifted by $0.05\boldsymbol{\sigma}$. We perform PCA on the data and monitor all PCs separately.

Figure 4 shows the control charts for top 5 and bottom 5 of PCs. As shown in the figure (left), the top PCs fail to detect the change. As mentioned earlier, this is due to the fact that top PCs have large variances, which make them insensitive to small shifts in the mean. On the other hand, the bottom PCs with smaller variances are more sensitive and can detect the small shift at the time it occurs, i.e., $t = 50$. This experiment was repeated several times, and each time similar results were found.

This shows that depending on the direction and the size of a change, the traditional approach of selecting top PCs may severely underperform. Therefore, it is imperative to develop a PC selection approach that can adaptively select the set of most sensitive PCs and does not depend on the a priori knowledge about the direction of the change.

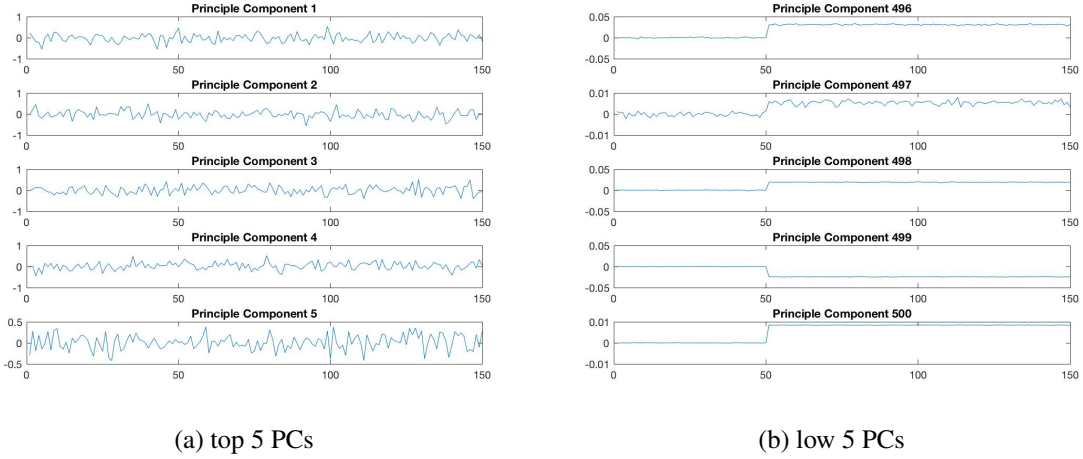


Figure 4: Comparing the behavior of top and low PCs for monitoring when a sparse shift happens in a random set of process of variables

2.2 Adaptive PC selection (APC) for Process Monitoring

In this section, we propose an adaptive PC Selection approach for process monitoring. This approach selects and monitors a set of PCs that show a higher deviation from a known in-control state. Suppose, the in-control observations follow $\mathbf{x}_t \sim N(\mathbf{0}, \Sigma); t < \tau$, and at an unknown time τ a mean shift occurs such that $\mathbf{x}_t \sim N(\boldsymbol{\mu}, \Sigma); t \geq \tau$, where, $\boldsymbol{\mu}$ is a non-zero sparse vector, and the process covariance is assumed to remain constant. Therefore, given the eigenvector matrix $A \in \mathbb{R}^{p \times p}$, the PC scores after the process change will become $\mathbf{y}_t = A^T \mathbf{x}_t \sim N(A^T \boldsymbol{\mu}, \Lambda)$, where $\Lambda = \text{diag}(\lambda_1, \lambda_2, \dots, \lambda_p)$.

The standardized expected shift magnitude along the j^{th} PC can be obtained by $\delta_j = \frac{\|\boldsymbol{\mu}\| \cos \theta_j}{\sqrt{\lambda_j}}; j = 1, 2, \dots, p$, where θ_j is the angle between the shift direction and the j^{th} PC. As can also be seen from Figure 2, this can imply that a PC closer to the shift direction (i.e. smaller θ) will capture a larger shift magnitude. Moreover, if θ is similar for two PCs, then the one with the smaller variance will be more sensitive to the change. Therefore, to take both measures into account, we work with standardized PC score, denoted by $\tilde{y}_{tj} = \frac{y_{tj}}{\sqrt{\lambda_j}}$, that contains both magnitude and sensitivity information.

We choose the EWMA statistic for monitoring as it is more sensitive to small changes and includes the information of previous samples. The EWMA statistic, denoted by z_{tj} , is defined as $z_{tj} = \gamma \tilde{y}_{tj} + (1 - \gamma) z_{(t-1)j}; t = 1, 2, \dots; j = 1, 2, \dots, p$, where $z_0 = 0$, and $\gamma \in [0, 1]$ is a weight.

Under the in-control process, $z_{tj} \sim N\left(0, \sigma^2 = \frac{\gamma}{1-\gamma}\right)$. Consequently, its squared standardized value follows a Chi-squared distribution with one degree of freedom, i.e., $d_{tj} = \left(\frac{z_{tj}}{\sqrt{\frac{\gamma}{1-\gamma}}}\right)^2 \sim \chi_{(1)}^2$.

When the process is out-of-control, depending on the direction of the mean shift, a few d_{tj} values will inflate, while the rest are slightly affected (or unaffected) by the mean shift. To increase the detection power of the monitoring procedure, these PCs should be filtered out. For this purpose, following Wang and Mei (2013), we use a soft-thresholding operator to define the following aggregated monitoring statistics,

$$R_t = \sum_{j=1}^p (d_{tj} - \nu)_+, \quad (1)$$

where the operator $(\cdot)_+ = \max\{0, \cdot\}$, and ν is the threshold value selected based on a desired significance level of χ^2 test. We monitor the R_t statistic and raise an alarm if, $R_t > R_0$, where R_0 is the threshold level found for a desired in-control ARL using simulations.

Selection of Control Limit (R_0)

To determine an appropriate value of R_0 , we require the distribution of monitoring statistic R . To find the distribution, we first specify the moments of thresholded values in Proposition 2.1.

Proposition 2.1. *If $d_{tj} \sim \chi_1^2$, then their soft thresholded values $\tilde{d}_{tj} = (d_{tj} - \nu)_+$ follows a bimodal truncated χ_1^2 distribution, with the following moments*

$$E(\tilde{d}_{tj}) = E((d_{tj} - \nu)_+) = \frac{1}{\Gamma(0.5)} [\Gamma(0.5, \frac{\nu}{2} + e^{-\frac{\nu}{2}} \sqrt{2\nu})] - \nu P(\chi_1^2 > \nu)$$

$$E(\tilde{d}_{tj}^2) = E((d_{tj} - \nu)_+^2) = \frac{1}{\Gamma(0.5)} [3\Gamma(0.5, \frac{\nu}{2} + e^{-\frac{\nu}{2}} \sqrt{2\nu})(3 + \nu)] - 2\nu E(\tilde{d}) - \nu^2 P(\chi_1^2 > \nu)$$

Proof is provided in Appendix A.

Using the Central Limit Theorem, $R \sim N(p\mu_{\tilde{d}}, \sqrt{p}\sigma_{\tilde{d}})$. Hence, R_0 for a desired type I error, α , is

$$R_0 = p\mu_{\tilde{d}} + \sqrt{p}\sigma_{\tilde{d}}\Phi^{-1}(1 - \alpha), \quad (2)$$

where Φ is the inverse normal cdf. To validate this approach and the normal approximation, we perform simulations in Section 3.1. The results show that the empirical α obtained by this approach is very close to the true α .

2.3 PC-based Signal Recovery (PCSR) Diagnosis Methodology

In monitoring high-dimensional data streams, apart from quick detection of changes, precise fault diagnosis to identify accountable variables is extremely crucial. Diagnosis aims at isolating the shifted variables, which will help identify and eliminate the root causes of a problem. However, despite its importance, very few diagnostic methods exist for high-dimensional data streams that is integrable with a PCA-based monitoring.

To that end, we propose a diagnostics approach that seamlessly integrates with the proposed PCA-based monitoring for large data streams. Inspired by Compressed Sensing (CS), we develop an adaptive lasso formulation to recover the variables responsible for an out-of-control alarm. We assume that only the process mean has shifted and the shift is sparse.

In CS, a high-dimensional sparse original signal can be reconstructed from noisy transformed observations by finding solutions to an underdetermined linear system. In other words, given a set of observations \mathbf{y} , and a transformation (sensing) matrix Υ , a sparse unknown original signal $\boldsymbol{\mu}$ can be recovered from $\mathbf{y} = \Upsilon\boldsymbol{\mu} + \boldsymbol{\varepsilon}$, where $\boldsymbol{\varepsilon}$ denotes the random errors.

The outcome of a PC monitoring method can be formulated similarly to identify the shifted process variables. Without loss of generality, we suppose the process has mean $\mathbf{0}$ during in-control that changes to a sparse mean $\boldsymbol{\mu}$ during the out-of-control of state. Therefore, the out-of-control observations follow $\mathbf{x} = \boldsymbol{\mu} + \boldsymbol{\varepsilon}$, where $\boldsymbol{\varepsilon} \sim (\mathbf{0}, \Sigma)$. Consequently, the out-of-control PC scores are,

$$\mathbf{y} = A\mathbf{x} = A\boldsymbol{\mu} + \tilde{\boldsymbol{\varepsilon}}, \quad (3)$$

where, $\tilde{\boldsymbol{\varepsilon}} = A\boldsymbol{\varepsilon}$ is the noise in the PC domain, with zero mean and covariance of $\Lambda = \text{diag}(\lambda_1, \lambda_2, \dots, \lambda_p)$.

Looking at Eq. 3, we can notice its similarity with a compressed sensing problem. In Eq. 3, the eigenvector matrix, A , and the principal scores, \mathbf{y} , are known, and we wish to estimate the shifted mean $\boldsymbol{\mu}$ when an out-of-control situation is detected after monitoring. Candes and Tao (2005) and Haupt and Nowak (2006) showed that a least squares objective function with L_1 penalty, also known as lasso, can be used to estimate the sparse vector $\boldsymbol{\mu}$. Since lasso estimates in general are not consistent, we use adaptive lasso Zou (2006) to build our diagnosis model.

Specifically,

$$\hat{\boldsymbol{\mu}} = \underset{\boldsymbol{\mu}}{\operatorname{argmin}} \{ \|\mathbf{y} - A\boldsymbol{\mu}\|_{l_2}^2 + r \sum_{j=1}^p w_j |\mu_j| \}, \quad (4)$$

where r is a nonnegative regularization parameter and $\mathbf{w} = \frac{1}{\hat{\mu}_{OLS}}$ is the data dependent weight vector.

One problem in solving Eq.4 is that the covariance matrix of $\boldsymbol{\varepsilon}'$ is not homogeneous. The variance heterogeneity may affect the estimation performance. To address this issue, we apply the following transformation to get constant variances for all error terms.

$$\mathbf{y}^* = \Lambda^{-\frac{1}{2}} \mathbf{y}, \quad A^* = \Lambda^{-\frac{1}{2}} A, \quad \boldsymbol{\varepsilon}^* = \Lambda^{-\frac{1}{2}} \boldsymbol{\varepsilon}'. \quad (5)$$

Consequently Eq. 3 is transformed to $\mathbf{y}^* = A^* \boldsymbol{\mu} + \boldsymbol{\varepsilon}^*$, where $\boldsymbol{\varepsilon}^* \sim (\mathbf{0}, \mathbf{I})$ with \mathbf{I} as a p dimensional identity matrix. The updated adaptive lasso formulation is given by.

$$\hat{\boldsymbol{\mu}} = \underset{\boldsymbol{\mu}}{\operatorname{argmin}} \{ \|\mathbf{y}^* - A^* \boldsymbol{\mu}\|_{l_2}^2 + r \sum_{j=1}^p w_j |\mu_j| \} \quad (6)$$

Where $w_j = 1/|\hat{\mu}_j|$, and $\hat{\boldsymbol{\mu}}$ is a root p -consistent estimator to $\boldsymbol{\mu}$, e.g., $\hat{\boldsymbol{\mu}} = \hat{\boldsymbol{\mu}}_{OLS}$. The optimization problem in Eq. 6 can be solved using various optimization algorithms, such as gradient descent, proximal descent, and LARS. In our implementation, we used the gradient descent method.

After finding the solution, the set of variables whose corresponding estimated μ_j is non-zero is considered as the altered variables. It should be noted that according to Theorem 2 in Zou (2006), the estimated mean is consistent, loosely meaning that when \mathbf{A}^* has large dimension (i.e. large p), the non-zero components of $\boldsymbol{\mu}$ are correctly identified. This implies that the larger the number of data streams the higher is the likelihood of correct diagnosis. See Appendix B for more details.

To determine the value of parameter r , one can use Bayesian Information Criterion (BIC) (Schwarz et al. (1978)) and choose the r value that results in the smallest BIC value. The reason behind choosing BIC is that it can determine the true sparse model if the true model is included in the candidate set (Yang (2005)). Since, in the diagnosis problem the objective is to detect

the nonzero elements (shifted variables) rather than estimation of the out-of-control mean, BIC is a proper criterion for diagnosis Zou et al. (2011).

3 Experimental Analysis

In this section, first we validate Proposition 2.1 using simulations. Afterwards, we study the performance of the proposed monitoring-diagnostic method in change detection and in terms of quick detection of mean shifts and identification of altered variables. For all the experiments, we simulate data streams such that in-control data follows a multivariate normal distribution $N(\mathbf{0}, \Sigma)$ and the out-of-control is $N(\boldsymbol{\mu}_1, \Sigma)$, $\boldsymbol{\mu}_1$ is sparse. We carry out the simulations for different levels and types of shifts and the covariance structure and compare the results with existing methods as benchmarks.

3.1 Validation of Proposition 2.1 for Choosing Control Limits

To validate Proposition 2.1, we perform two sets of experiments. In the first experiment, we generate $d_j \sim \chi_1^2$ for $j = 1, \dots, p$, and $R_t = \sum_{j=1}^p (d_{tj} - \nu)_+$ for $t = 1, \dots, 1000$, similar to Eq. 1. Then we calculate R_0 using Eq. 2 for desired $\alpha = 0.05$. We calculate the empirical Type I error, denoted by $\tilde{\alpha}$, as the fraction of times R_t 's pass the control limit R_0 . We perform this experiment for different values of p and ν and replicate each scenario 1000 times. Finally, we report the average empirical Type I errors in table 1.

In the second experiment, first we simulate \mathbf{x}_t for $t = 1, \dots, 1000$ as a p dimensional normal distribution random variables with random covariance matrix and zero mean. Given the eigenvector matrix \mathbf{A} , we calculate its PC scores, and its corresponding EWMA statistic using $\gamma = 0.4$. Consequently, its squared standardized value are calculated as $d_{tj} = \left(\frac{z_{tj}}{\sqrt{\frac{\gamma}{1-\gamma}}} \right)^2$.

Here, for each observation we define $R_t = \sum_{j=1}^p (d_{tj} - \nu)_+$, we repeat this procedure 1000 times. Similar to previous experiment, we calculate R_0 using Eq. 2 for desired $\alpha = 0.05$. We calculate the empirical Type I error, $\tilde{\alpha}$, as the fraction of times R_t 's pass the control limit R_0 . We replicate each (p, ν) scenario 1000 times and we report the average empirical type I errors in table 2.

As can be seen from Table 1-2, as p increases, the empirical Type I error approaches to its true value $\alpha = 0.05$. Moreover, for large p , the result is less sensitive to the choice of the threshold value, v . Hence, it shows the validity of the proposed approach for finding control limits.

Note that the main difference between these studies is the independence of R_t 's. In the first study, R_t 's are independently generated, whereas in the second study, R_t 's are calculated using EWMA statistics, which are not independent. The larger bias in the results of the second study is mainly because the monitoring statistic values are autocorrelated. However, for very large p (e.g, $p > 5000$), this difference is negligible. For smaller p , we would suggest using a Monte Carlo simulation to determine the control limits.

Table 1: Empirical type I error using first experiment

		p				
		100	500	1000	5000	10000
v	0.05	0.0090	0.0067	0.0063	0.0056	0.0053
	0.10	0.0091	0.0067	0.0060	0.0055	0.0052
	0.15	0.0090	0.0067	0.0062	0.0056	0.0054
	0.20	0.0090	0.0066	0.0064	0.0055	0.0054
	0.25	0.0091	0.0068	0.0061	0.0055	0.0054
	0.35	0.0092	0.0068	0.0063	0.0055	0.0053

Table 2: Empirical type I error using second experiment

		p				
		100	500	1000	5000	10000
v	0.05	0.0091	0.0071	0.0068	0.0065	0.0050
	0.10	0.0091	0.0073	0.0067	0.0064	0.0050
	0.15	0.0090	0.0073	0.0067	0.0063	0.0050
	0.20	0.0091	0.0072	0.0067	0.0063	0.0051
	0.25	0.0089	0.0072	0.0068	0.0061	0.0049
	0.35	0.0083	0.0066	0.0063	0.0057	0.0047

3.2 Monitoring Methods Analysis

In this section, we conduct various simulations to validate the performance of the proposed monitoring method based on the Average Run Length (ARL) and its standard error for different magnitudes of shifts. Specifically, the following scenarios are considered:

I. Random covariance structure and random shift: To generate the random covariance matrix, we use the Wishart distribution with diagonal entries equal to 1. To generate a sparse mean shift, we randomly select 20% of the process variables and shift them by δ .

II. Block diagonal covariance: This scenario mimics the situations where each data stream is correlated with only a subset of the data streams. The covariance matrix used in this scenario has $K = 12$ blocks, denoted as $B_k, k = 1, \dots, K$. Each block B_k is a random semi-positive definite matrix generated from a Wishart distribution. To generate out-of-control data, we shift the mean of some of the variables that belong to only one of the blocks

$$(B_k), \text{ by } \delta, \text{ i.e., } \mu_j = \begin{cases} \delta & j \in B_k \\ 0 & j \notin B_k \end{cases}.$$

In each scenario, p data streams are generated. We run the simulations for, $p = 100, p = 1000,$ and $p = 10,000$ to evaluate the performances in different dimensions. We apply the proposed monitoring method, APC, and compare it with three existing methods:

a) T_{new} by Zou et al. (2015). This monitoring method is based on a goodness-of-fit test of the local CUSUM statistics from each data stream.

b) TRAS by Liu et al. (2015). Top-r based adaptive sampling (TRAS) is an adaptive sampling strategy that uses the sum of top-r local statistics for monitoring. Since this method works only for independent variables, we will implement it on PCs rather than original data,

c) Traditional PCA-based monitoring. In this approach, the selected number of components to retain in the model is based on the cumulative percentage of variance (CPV) equal to 90. Control charts are constructed by using the Hotelling's T^2 statistic and the Q statistic (De Ketelaere et al. (2015)).

To detect an out-of-control condition, the control limits are set such that the ARL for in-control observations is equal to 200 (this corresponds to a significance level of 0.005). Each control limit is calculated through 1,000 replications. The results are shown in Figures 5-7.

For $p = 100$, as shown in Figure 5(a), the proposed APC markedly outperforms the other benchmark methods. Even for shifts as small as $\delta = 0.1\sigma$, the ARL for APC is 4.06. This is about fourteen times smaller than the second best method, which is TRAS with ARL equal to 56. Moreover, for shifts $\delta \geq 0.1\sigma$, APC detects the shift almost instantly (i.e., $ARL_1 = 1$).

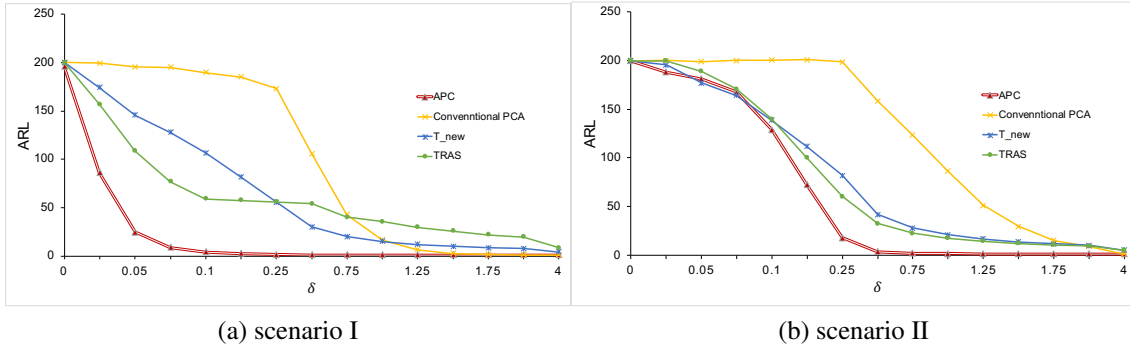


Figure 5: ARL of scenarios I, II for different values of δ (shift magnitude) for $p = 100$

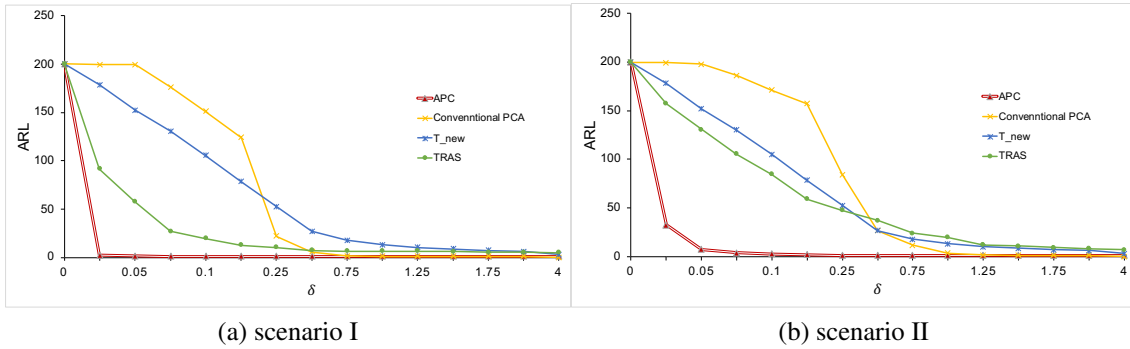


Figure 6: ARL of scenarios I, II for different values of δ (shift magnitude) for $p = 1000$

The results for Scenario II in Figure 5(b) also show that APC is superior to others, especially for moderate and large shifts. As an example, for a shift with the magnitude of $\delta = 0.25\sigma$, APC's ARL is 17.67, while this values for the best benchmark (TRAS) is 61.37. As expected, the out-of-control ARL values for all methods in Scenario II is larger than those in Scenario I.

For higher dimensions, the APC's ability to detect shifts becomes even better while the other method's performances stay the same or deteriorate. This shows that as dimension grows, the shifts are easier to be captured in PC scores that are in the direction of the shift.

To summarize, this study indicates that the APC method outperforms other methods for detecting small values of shifts. Also, as dimension grows APC works better in detecting a change promptly. This can be attributed to the adaptive nature of the proposed monitoring statistic.

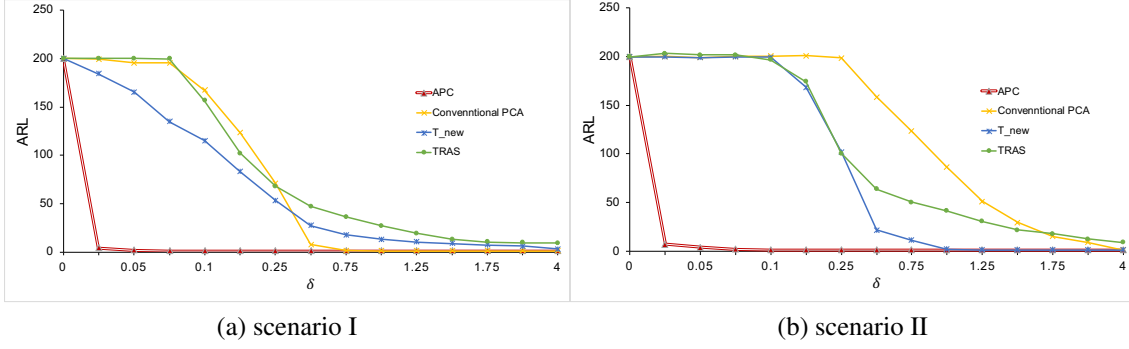


Figure 7: ARL of scenarios I, II for different values of δ (shift magnitude) for $p = 10,000$

3.3 Diagnosis Analysis

In this section, in addition to Scenarios I and II presented in the previous section, we add another scenario (Scenario III) with an autoregressive covariance matrix, i.e., $\rho_{ij} = |0.5|^{(i-j)}$ for variables i, j . This covariance matrix impose the variables close to each other to have higher covariance and as the variables go farther in the matrix, their covariance becomes smaller. We validate the performance of the proposed diagnosis method for different percentages of shifted variables (PS) as well as their shift magnitudes (δ), using the following performance measures: (a) false negative percentage (%FN), defined as the percentage of the number of variables that are not detected over the number of all faulty variables; (b) false positive percentage (%FP), defined as the percentage of the ratio of number of variables that are mistakenly detected as faulty over the number of all not-faulty variables; (c) parameter selection score (PSS), defined as the total number of variables that are labeled incorrectly (either as faulty or not-faulty); and (d) F1-Score, defined as the harmonic average of the precision and recall, and indicates our overall performance combining the FP and FN.

For FN, FP and PSS measures, the smaller the value, the better the performance, whereas for F1-score the higher the better. We compare the performance of our proposed method with the Lasso-based diagnosis approach proposed by Zou et al. (2011) called LEB. LEB is an LASSO-based diagnostic approach for diagnosis of sparse changes using BIC and the adaptive LASSO variable selection. The comparison results for $p = 100$ are shown in Tables 3-5, and Figures 8-10 for scenarios I, II, and III, respectively.

In these tables PS denotes the percentage of shifted process variables. As shown in Table 3

and Figure 8, under scenario I, when shift occurs in a random set of variables with a random covariance matrix, our proposed PCSR performs better than the LEB (Zou et al. (2011)) for most of the cases except for the case with PS=10% and small shifts (i.e., $\delta = 0.7\sigma$). Even in this case, PCST is close to LEB. However, for larger shifts, PCSR outperforms LEB. For instance, for a shift equal to 1σ and percentage of shifted variables equal to 10% the $F1$ accuracy using PCSR is equal to 0.9881 while it is equal to 0.9363 for LEB.

In Scenario II, PCSR clearly outperforms the LEB method. For example for a shift equal to 0.7σ on 10% of variables, PCSR's $F1$ -score is 0.6802 while, the LEB $F1$ score is 0.3725 (see Table 4 and Figure 9).

Also, the results in scenario III indicate the superior performance of that our method (see Table 5 and Figure 10). For instance, for a 0.5σ shift on 25% of variables, PCSR's $F1$ -score is 0.7173 and 0.4648 for LEB.

These results show that for random non-sparse covariance matrices, the LEB method and PCSR method performs almost similarly. However, for sparse covariance matrices such as a block covariance or an autoregressive covariance, PCSR clearly outperforms LEB method. These sparse occurrence of covariance matrices are very common in real world. This is because of the fact that in many situations, each data stream is correlated only with a small group of other data streams, but is not correlated with all other data streams collected in the system. Hence, a method that can detect the changes in such systems is necessary and more appropriate for real-world applications.

In sum, the results of the simulation study show the effectiveness of our method in identifying the set of altered variables and its superiority over the current state-of-the-art.

4 Case Study

In this section, we apply the proposed monitoring and diagnosis methods on two case studies, a) defect detection in a steel rolling process, and b) quality monitoring of wine. Additionally, we compare our results with the existing methods.

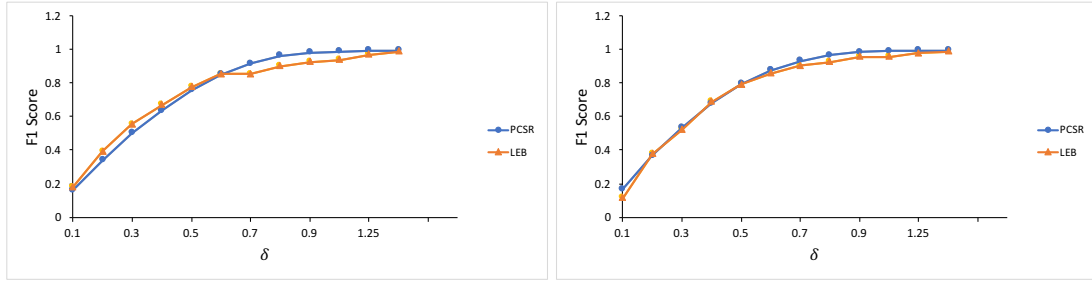
Shift	PCSR				LEB				
	FP%	FN%	PSS	F1	FP%	FN%	PSS	F1	
PS=0.1	0.1	86.99	5.289	13.459	0.1603	85.86	4.28	12.438	0.1790
	0.3	41.36	8.652	11.923	0.5001	38.11	6.757	9.891	0.5554
	0.5	8.05	6.107	6.301	0.757	6.56	5.501	5.607	0.7763
	0.7	0.62	2.272	2.107	0.9141	0.62	3.924	3.594	0.8538
	1	0	0.29	0.261	0.9881	0	1.580	1.422	0.9363
	1.25	0	0.1567	0.141	0.9934	0	0.761	0.685	0.968
	1.5	0	0.156	0.14	0.9935	0	0.347	0.312	0.9850
	PS=0.15	0.1	87.267	6.388	18.52	0.1672	92.067	3.466	16.756
0.3		42.773	10.231	15.112	0.5323	45.84	9.379	14.848	0.520
0.5		9.16	7.029	7.349	0.7927	8.853	7.077	7.343	0.7916
0.7		0.687	2.68	2.381	0.9310	0.433	3.914	3.392	0.9015
1		0	0.364	0.309	0.9903	0	1.711	1.454	0.9552
1.25		0	0.242	0.206	0.9935	0	0.854	0.726	0.9772
1.5		0	0.229	0.195	0.9938	0	0.439	0.373	0.9882
PS=0.25		0.1	86.676	7.303	27.146	0.1941	88.632	4.815	25.769
	0.3	48.268	10.277	19.775	0.5653	52.116	8.736	19.581	0.5460
	0.5	15.896	6.939	9.178	0.8208	19.848	6.372	9.741	0.8028
	0.7	1.228	3.123	2.649	0.9505	3.004	6.123	5.343	0.9018
	1	0	0.489	0.367	0.9929	0	3.145	2.359	0.956
	1.25	0	0.371	0.278	0.9946	0	1.876	1.407	0.9732
	1.5	0	0.368	0.276	0.9947	0	1.161	0.871	0.9832

Table 3: Diagnosis simulation results for Scenario I

4.1 Defect detection in Steel Rolling Process

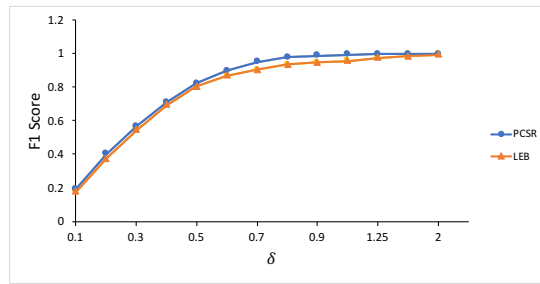
Early detection of process shifts in a rolling process is necessary to avoid damage to products and reduce manufacturing costs. Rolling is a high-speed process that makes its monitoring particularly challenging. In this study, we show that the PCA-based method can effectively detect anomalies and damages imprinted on a steel bar after rolling. The dataset we consider here, includes images of size 128×512 pixels of the surface of rolled bars collected by a high-speed camera Yan et al. (2017). Of the 100 images, the first 50 images are in-control. One example of the image of rolling data for in-control vs out-of-control process is shown in Figure 11.

We use this data to simulate an image with in-control observations in the first 126 rows and out-of-control observations in the remaining 72 rows. The generated image is presented in Figure 12. Also, we crop the image at the right end to avoid the non-informative dark segment of the image. Hence, our generated picture is of the size of 198×300 . In this study, each row of an image (a vector of 300×1) is treated as an observation, creating a multi-stream data with



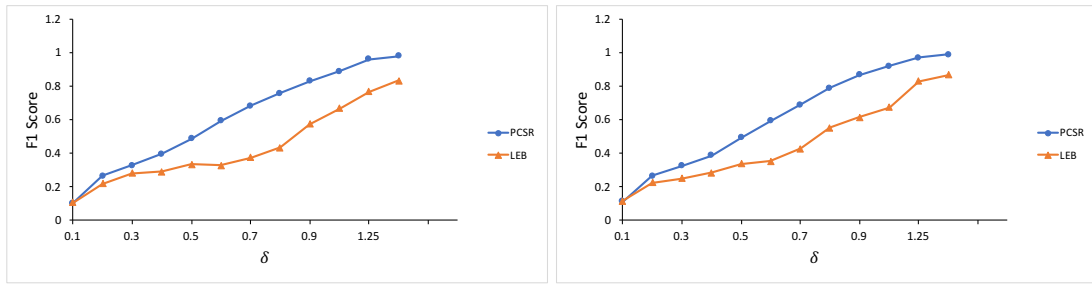
(a) PS=0.10

(b) PS=0.15



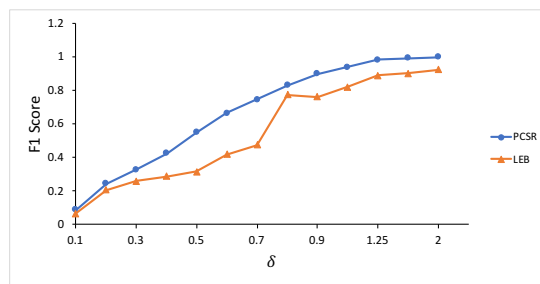
(c) PS=0.25

Figure 8: F1 of scenarios I different values of δ (shift magnitude)



(a) PS=0.10

(b) PS=0.15



(c) PS=0.25

Figure 9: F1 of scenarios II different values of δ (shift magnitude)

the size of 300. As the picture shows, for out-of-control observations, some small black lines, indicating anomalies, emerge at the left part of the frame. We are interested to see whether our

PS	Shift	PCSR				LEB			
		%FP	%FN	PSS	F1	%FP	%FN	PSS	F1
PS=0.10	0.1	93.775	0.40435	7.874	0.1011	93.663	0.91304	8.333	0.1049
	0.3	78.412	0.5337	6.764	0.3257	81.562	0.93478	7.385	0.2784
	0.5	63.1	0.75652	5.744	0.4854	76.987	0.81848	6.912	0.3333
	0.7	40.387	1.0446	4.192	0.6802	72.162	0.96848	6.664	0.3725
	1	8.575	1.2109	1.8	0.8875	33.562	2.4522	4.941	0.6672
	1.25	0.7375	0.71413	0.716	0.9586	12.425	3.5022	4.216	0.7664
	1.5	0	0.40217	0.37	0.9789	0.6625	3.612	3.376	0.8302
PS=0.15	0.1	93.537	0.50714	15.392	0.1119	93.419	0.75476	15.581	0.1160
	0.3	79.588	0.69405	13.317	0.3225	84.9	1.1179	14.523	0.2475
	0.5	64.444	0.98333	11.137	0.4925	77.825	1.3536	13.589	0.3355
	0.7	42.219	1.3167	7.861	0.6891	68.863	1.7393	12.479	0.4258
	1	7.8375	1.519	2.53	0.9182	39.062	2.9917	8.763	0.6712
	1.25	0.81875	1.0476	1.011	0.9696	7.0625	5.8714	6.062	0.8282
	1.5	0.00625	0.52262	0.44	0.9869	0.225	5.969	5.05	0.8662
PS=0.25	0.1	95.088	0.56447	23.25	0.0878	96.525	0.87105	23.828	0.0641
	0.3	79.483	1.0329	19.861	0.3251	84.133	1.5408	21.363	0.2593
	0.5	59.008	1.7592	15.499	0.5489	80.083	1.3763	20.266	0.3140
	0.7	36.492	1.7855	10.115	0.7440	64.933	2.2645	17.305	0.4742
	1	6.4167	1.8013	2.909	0.9379	15.758	6.4645	8.695	0.8180
	1.25	0.57083	1.1645	1.022	0.9792	2.625	7.0224	5.967	0.8878
	1.5	0.0083333	0.62895	0.48	0.9903	0.1	7.1421	5.452	0.8993

Table 4: Diagnosis simulation results for Scenario II

monitoring approach can detect this change, and whether the diagnosis approach can determine the changed pixels.

Monitoring. We apply our proposed APC method for monitoring the process. We use the first 70 in-control data (the first 70 rows of the image) to obtain the control limits. The control limits are determined according to the procedure explained in Sec. 3.2 to achieve the in-control ARL of 200. The resulting control chart is shown in Figure 13. As can be seen from the figure, after the change point, our monitoring statistic instantly inflates and raises an out-of-control alarm by the first observation after the change. Furthermore, to compare its performance with existing state-of-the-art methods, we report the run lengths (the number of observations before the change is detected) for each method in Table 6. In the results, APC has the smallest run-length (RL). This implies APC is the fastest in detecting the change in comparison to other benchmarks.

Diagnosis. To check the performance of our PCSR method, we performed diagnosis using

Shift		PCSR				LEB			
		%FP	%FN	PSS	F1	%FP	%FN	PSS	F1
PS=0.10	0.1	98.48	0.63667	10.421	0.0257	97.31	0.87222	10.516	0.0484
	0.3	82.78	0.85778	9.05	0.2562	92.08	0.47667	9.637	0.1385
	0.5	38.18	1.1511	4.854	0.7073	73.69	0.40889	7.737	0.3675
	0.7	7.44	1.0178	1.66	0.9176	17.54	1.4233	3.035	0.8303
	1	0.11	0.61556	0.565	0.9740	0.38	0.94444	0.888	0.9595
	1.25	0	0.60111	0.541	0.9752	0.02	0.67	0.605	0.9722
	1.5	0	0.46889	0.422	0.9806	0	0.62444	0.562	0.9742
PS=0.15	0.1	98.347	0.6259	15.284	0.0293	97.513	0.84824	15.348	0.0460
	0.3	81.48	1.0471	13.112	0.2832	91.853	0.31059	14.042	0.1431
	0.5	35.48	1.4965	6.594	0.7390	56.067	0.77882	9.072	0.5457
	0.7	6.5533	1.2553	2.05	0.9319	10.033	1.9471	3.16	0.8924
	1	0.11333	0.64706	0.567	0.9821	0.19333	1.6247	1.41	0.9567
	1.25	0	0.60824	0.517	0.9837	0	0.96471	0.82	0.9744
	1.5	0	0.60941	0.518	0.9836	0	0.68	0.578	0.9818
PS=0.25	0.1	98.564	0.64533	25.125	0.0264	98.312	0.86	25.223	0.0323
	0.3	83.508	1.184	21.765	0.2641	93.74	0.272	23.639	0.1128
	0.5	40.056	1.86	11.409	0.7173	63.888	1.124	16.815	0.4648
	0.7	8.856	1.604	3.417	0.9292	13.84	3.1027	5.787	0.8776
	1	0.184	0.78	0.631	0.9878	0.348	2.7707	2.165	0.9593
	1.25	0.004	0.65333	0.491	0.9905	0.008	1.8747	1.408	0.9732
	1.5	0	0.60133	0.451	0.9913	0	1.1693	0.877	0.9831

Table 5: Diagnosis simulation results for Scenario III

our method vs LEB method on the out of control data. The phase-1 data is used as the ground truth (sample size 70), and 25 out-of-control observations are used to detect the changed pixels in the generated image. The area selected as out-of-control for each method as well as the in-control and out-of-control images are shown in Figure 14. The identified pixels are shown in black and the remaining unchanged pixels are shown in white in Figure 14(c) and (d), respectively.

As the results show, PCSR method clearly detects the changed pixels in the image with no false detection. Note that although LEB can identify the changed pixels, it generates a few false detection areas.

4.2 Wine Quality Monitoring

In this section, we demonstrate the efficacy of our proposed methodology by applying it to a real dataset from a white wine production process. The data is taken from the UCI data

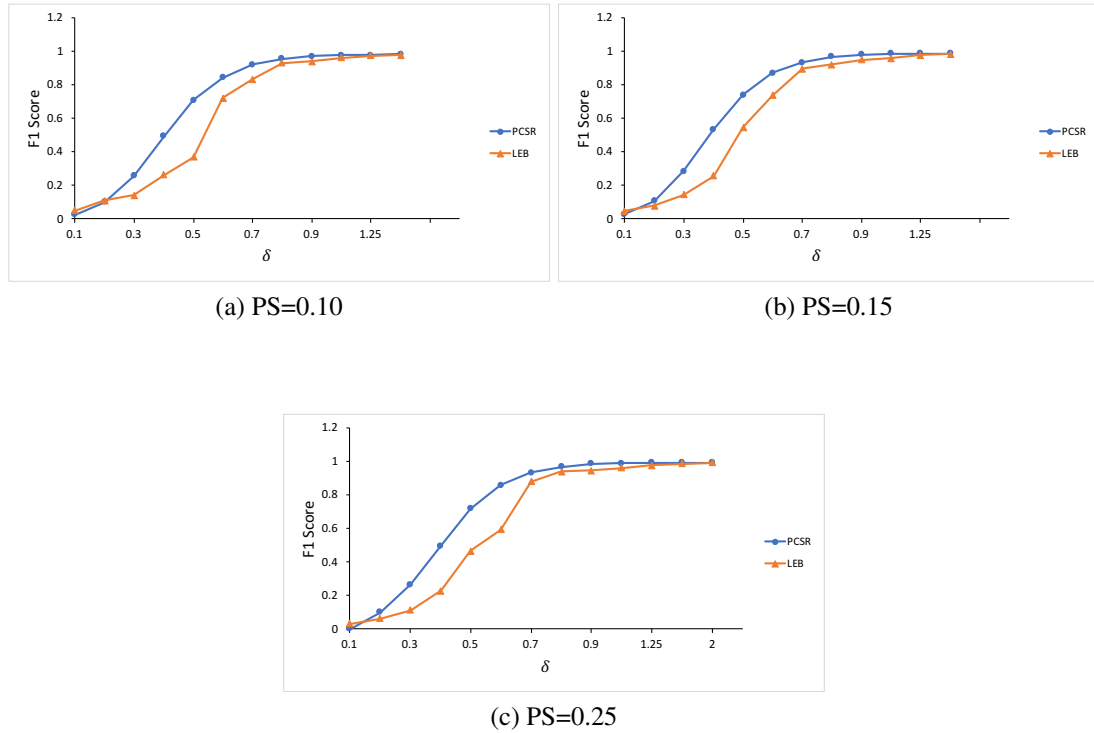


Figure 10: F1 of scenarios III different values of δ (shift magnitude)

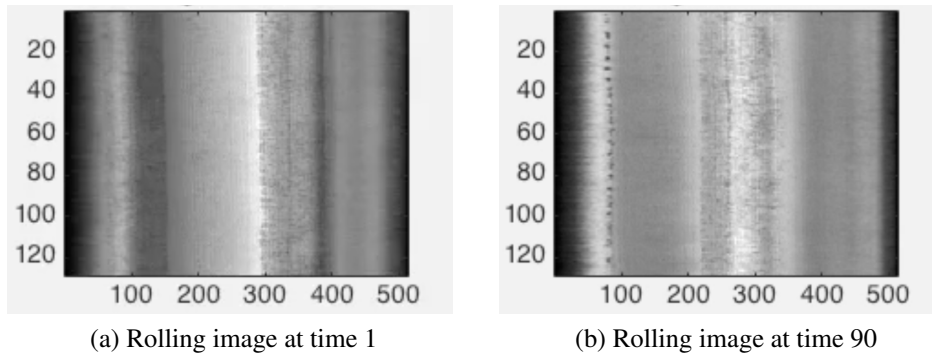


Figure 11: Image of rolling data for in control process (a) and out of control process (b)

repository¹. The data has 4898 observations obtained between May 2004 to February 2007 for the purpose of improving the quality of Portuguese Vinho Verde wine. The collected data has eleven variables named as fixed acidity, volatile acidity, citric acid, residual sugar, chlorides, free sulfur dioxide, total sulfur dioxide, density, PH, sulphates and alcohol. An additional (manually annotated) quality variable is available that will be used as ground truth for the wine quality. This variable ranges between 0 (very bad) and 10 (very excellent), and is provided based on sensory analysis Cortez et al. (2009).

Our objective is to monitor the wine quality using the variables and diagnose the shifted

¹<http://archive.ics.uci.edu/ml/datasets/Wine+Quality>



Figure 12: Generated Image with first 126 rows (from the top) as in-control and remaining 72 rows as out-of-control

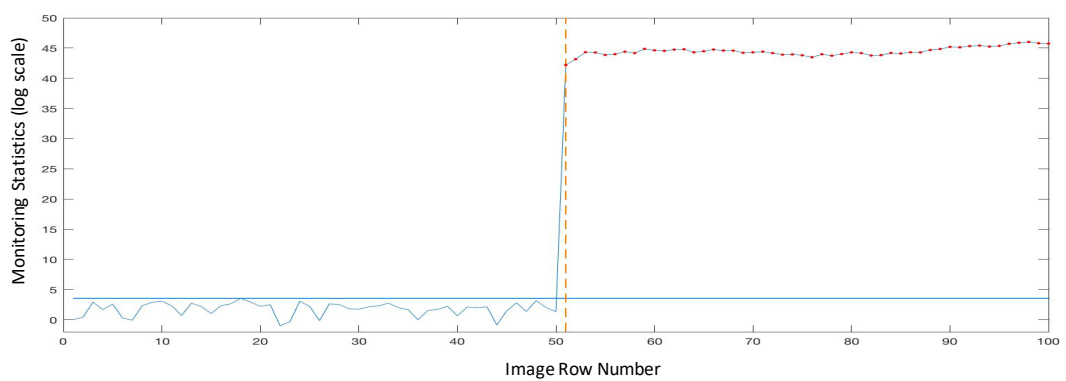
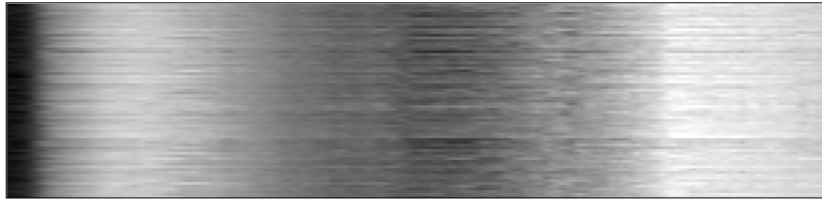
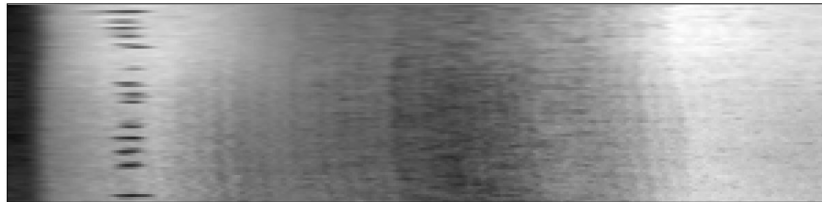


Figure 13: Monitoring Rolling Data using APC Method



(a) In-control image



(b) Out-of-control image



(c) Diagnosis using PCSR



(d) Diagnosis using LEB

Figure 14: Diagnosis using PCSR and LEB method

Method	Detected Change Point
APC	1
Conventional PCA	16
T_new (Zou et al. (2015))	10
TRAS (Liu et al. (2015))	14

Table 6: Run length Comparison of different methods in detecting the change point

Method	N_A =Number of observations after Chang point until alarm
APC	11
Conventional PCA	23
T_new Zou et al. (2015)	24
TRAS Liu et al. (2015)	28

Table 7: Comparison of different methods in detecting the change

variables, if there is a shift. We perform the APC study on this dataset. Similar to Zou et al. (2015)’s study on this data, we focus on a subset of the data in which the quality variable is either 6 or 7. The observations with the quality of 7 are considered as acceptable while the rest are unacceptable, hence out-of-control. The quality variable is the ground truth that is used to gauge the performance of our monitoring—the monitoring should raise an out-of-control alarm as soon as the quality variable is going down from 7 to 6. When the alarm is raised, our diagnosis approach should be able to pinpoint the actual shifted process variables.

Monitoring. Overall there are 880 observations with the quality equal to 7 of which 830 observations are used for phase I monitoring. Also, we set the control limits (R_0 in APC method) such that ARL for in-control observation is 1000. To do the comparison, we implement our method along with the existing methods shown in Sec. 3.2. All parameters in the methods are set to achieve in-control ARL of 1000 so that the methods are comparable.

For phase II monitoring, we use the remaining 40 points with the quality of 7 followed by observations with the quality of 6. The goal is to investigate how fast and accurately our monitoring algorithm detects the change point in comparison to the existing methods.

The results are shown in Table 7 and Figure 15. As shown in Table 7, the APC monitoring method detects the change after 11 observations. On the other hand, other methods took more than twice as many observations to detect the change.

Diagnosis. Among the eleven variables, four were determined as shifted variables by

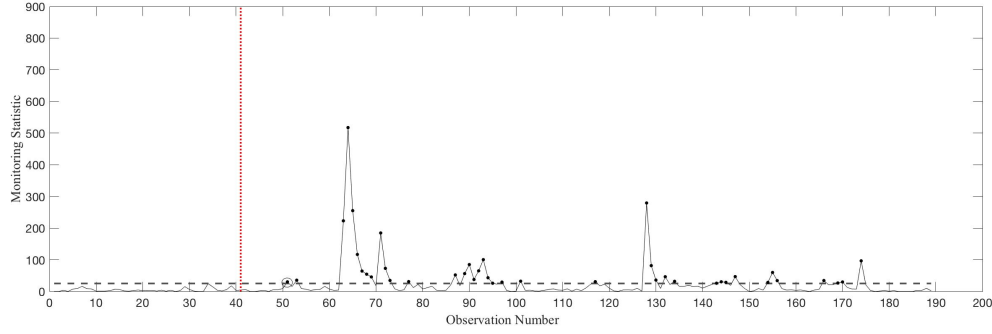


Figure 15: Monitoring Wine Quality Data using APC Method

PCSR, viz. residual sugar, chlorides, density, and alcohol. The LEB method selected chlorides, density and alcohol as the shifted variables.

5 Conclusion

In this paper, we proposed an SPC framework for high-dimensional data streams that seamlessly integrates monitoring and diagnostics. We proposed a new PCA-based monitoring approaches, viz. Adaptive PC Selection (APC) monitoring. We first negated the common belief that the high-PCs (principal components with highest variances) should be used for monitoring, and then, showed that monitoring adaptively selected PCs will be more effective. Using simulations, we showed that adaptively selected PCs outperforms other benchmark methods for different types of covariance matrix structures and types of shifts. Moreover, in all the stated scenarios, the conventional approach of monitoring high-PC was shown to have poorer performance.

In the diagnosis module, we first discussed the challenge in finding the shifted variables after a PCA-based monitoring procedure. The challenge lies in isolating the process variable from the signaling PC. To address this, we used the CS principle to formulate an adaptive Lasso estimation to detect the shifted variables. This formulation takes the eigenvectors and principal components (after a shift) as inputs and yields the process variables that caused the shift. Our experimental validations showed that the proposed PCSR performs significantly better than the current state-of-the-art.

Furthermore, we showed the practical applicability and validity of our methods via real-

world case studies. The first case study was on defect detection in a steel rolling process, in which we found that the proposed APC detects the shift faster than all the other methods. Moreover, the PCSR diagnosis approach detects the change pixels better than the existing method with fewer false positives. In another case study, we monitored wine quality and diagnosed the shift. Our monitoring approach was again faster and our diagnosis approach could find an additional shifted process variable, *sugar*, that was undetected by the existing diagnostics approach.

In this paper, we have focused on monitoring and diagnosing the mean shifts. While the developed APC can potentially be used to detect shifts in covariances, further research is required to extend the PCSR diagnostics approach to the covariance matrix monitoring.

References

- Alcala, C. F. and Qin, S. J. (2009). Reconstruction-based contribution for process monitoring. *Automatica*, 45(7):1593–1600.
- Candes, E. J. and Tao, T. (2005). Decoding by linear programming. *IEEE transactions on information theory*, 51(12):4203–4215.
- Capizzi, G. and Masarotto, G. (2011). A least angle regression control chart for multidimensional data. *Technometrics*, 53(3):285–296.
- Cortez, P., Cerdeira, A., Almeida, F., Matos, T., and Reis, J. (2009). Modeling wine preferences by data mining from physicochemical properties. *Decision Support Systems*, 47(4):547–553.
- De Ketelaere, B., Hubert, M., and Schmitt, E. (2015). Overview of pca-based statistical process monitoring methods for time-dependent, high-dimensional data. *Journal of Quality Technology*, 47:318–335.
- Dunia, R. and Joe Qin, S. (1998). Subspace approach to multidimensional fault identification and reconstruction. *AIChE Journal*, 44(8):1813–1831.

- Haupt, J. and Nowak, R. (2006). Signal reconstruction from noisy random projections. *IEEE Transactions on Information Theory*, 52(9):4036–4048.
- Jackson, J. E. and Mudholkar, G. S. (1979). Control procedures for residuals associated with principal component analysis. *Technometrics*, 21(3):341–349.
- Joe Qin, S. (2003). Statistical process monitoring: basics and beyond. *Journal of chemometrics*, 17(8-9):480–502.
- Li, G., Qin, S. J., and Zhou, D. (2014). A new method of dynamic latent-variable modeling for process monitoring. *IEEE Transactions on Industrial Electronics*, 61(11):6438–6445.
- Li, W., Yue, H. H., Valle-Cervantes, S., and Qin, S. J. (2000). Recursive pca for adaptive process monitoring. *Journal of process control*, 10(5):471–486.
- Liu, K., Mei, Y., and Shi, J. (2015). An adaptive sampling strategy for online high-dimensional process monitoring. *Technometrics*, 57(3):305–319.
- MacGregor, J. F., Jaeckle, C., Kiparissides, C., and Koutoudi, M. (1994). Process monitoring and diagnosis by multiblock pls methods. *AIChE Journal*, 40(5):826–838.
- Mei, Y. (2010). Efficient scalable schemes for monitoring a large number of data streams. *Biometrika*, 97(2):419–433.
- Mei, Y. (2011). Quickest detection in censoring sensor networks. In *Information Theory Proceedings (ISIT), 2011 IEEE International Symposium on*, pages 2148–2152. IEEE.
- Qahtan, A. A., Alharbi, B., Wang, S., and Zhang, X. (2015). A pca-based change detection framework for multidimensional data streams: Change detection in multidimensional data streams. In *Proceedings of the 21th ACM SIGKDD International Conference on Knowledge Discovery and Data Mining*, pages 935–944. ACM.
- Qin, S. J., Valle, S., and Piovoso, M. J. (2001). On unifying multiblock analysis with application to decentralized process monitoring. *Journal of chemometrics*, 15(9):715–742.

- Schwarz, G. et al. (1978). Estimating the dimension of a model. *The annals of statistics*, 6(2):461–464.
- Sparks, R. S. (1992). Quality control with multivariate data. *Australian & New Zealand Journal of Statistics*, 34(3):375–390.
- Sullivan, J. H., Stoumbos, Z. G., Mason, R. L., and Young, J. C. (2007). Step-down analysis for changes in the covariance matrix and other parameters. *Journal of Quality Technology*, 39(1):66.
- Tamura, M. and Tsujita, S. (2007). A study on the number of principal components and sensitivity of fault detection using pca. *Computers & Chemical Engineering*, 31(9):1035–1046.
- Tartakovsky, A. G., Rozovskii, B. L., Blažek, R. B., and Kim, H. (2006). Detection of intrusions in information systems by sequential change-point methods. *Statistical methodology*, 3(3):252–293.
- Wang, K. and Jiang, W. (2009). High-dimensional process monitoring and fault isolation via variable selection. *Journal of Quality Technology*, 41(3):247.
- Wang, Y. and Mei, Y. (2013). Monitoring multiple data streams via shrinkage post-change estimation. *Annals of Statistics*.
- Westerhuis, J. A., Gurden, S. P., and Smilde, A. K. (2000). Generalized contribution plots in multivariate statistical process monitoring. *Chemometrics and intelligent laboratory systems*, 51(1):95–114.
- Wierda, S. J. (1994). Multivariate statistical process control-recent results and directions for future research. *Statistica Neerlandica*, 48(2):147–168.
- Wise, B. M., Ricker, N., Veltkamp, D., and Kowalski, B. R. (1990). A theoretical basis for the use of principal component models for monitoring multivariate processes. *Process control and quality*, 1(1):41–51.
- Yan, H., Paynabar, K., and Shi, J. (2017). Anomaly detection in images with smooth background via smooth-sparse decomposition. *Technometrics*, 59(1):102–114.

- Yang, Y. (2005). Can the strengths of aic and bic be shared? a conflict between model identification and regression estimation. *Biometrika*, 92(4):937–950.
- Yuan, L. and Xiao-Chu, T. (2009). Improved performance of fault detection based on selection of the optimal number of principal components. *Acta Automatica Sinica*, 35(12):1550–1557.
- Yue, H. H. and Qin, S. J. (2001). Reconstruction-based fault identification using a combined index. *Industrial & engineering chemistry research*, 40(20):4403–4414.
- Zou, C., Jiang, W., and Tsung, F. (2011). A lasso-based diagnostic framework for multivariate statistical process control. *Technometrics*, 53(3):297–309.
- Zou, C. and Qiu, P. (2009). Multivariate statistical process control using lasso. *Journal of the American Statistical Association*, 104(488):1586–1596.
- Zou, C., Wang, Z., Zi, X., and Jiang, W. (2015). An efficient online monitoring method for high-dimensional data streams. *Technometrics*, 57(3):374–387.
- Zou, H. (2006). The adaptive lasso and its oracle properties. *Journal of the American statistical association*, 101(476):1418–1429.

A First and second moments of the thresholded statistic

The first moment of \tilde{d} is calculated as,

$$\begin{aligned}
E(\tilde{d}) &= E((d_{tj} - \nu)_+) = E((d_{tj} - \nu) | d_{tj} > \nu) P(d_{tj} > \nu) \\
&= E((d_{tj} | d_{tj} > \nu) p(d_{tj} > \nu) - \nu P(d_{tj} > \nu) \\
&= \int_{\nu}^{\infty} dP(d) - \nu P(\chi_1^2 > \nu) \\
&= \int_{\nu}^{\infty} \left\{ x \frac{1}{\sqrt{2}\Gamma(0.5)} x^{-\frac{1}{2}} e^{-\frac{x}{2}} \right\} dx - \nu P(\chi_1^2 > \nu) \\
&= \frac{1}{\Gamma(0.5)} \left\{ \Gamma\left(0.5, \frac{\nu}{2}\right) + e^{-\frac{\nu}{2}} \sqrt{2\nu} \right\} - \nu P(\chi_1^2 > \nu)
\end{aligned} \tag{7}$$

To calculate the second moment of \tilde{d} ,

$$\begin{aligned}
E(\tilde{d}^2) &= E((d_{tj} - \nu)_+^2) = E((d_{tj} - \nu)_+^2 | d_{tj} > \nu) P(d_{tj} > \nu) \\
&= E(d_{tj}^2 | d_{tj} > \nu) P(d_{tj} > \nu) - 2\nu E(d_{tj} | d_{tj} > \nu) P(d_{tj} > \nu) + \nu^2 P(d_{tj} > \nu) \xrightarrow{\text{Eq.7}} \\
&= \int_{\nu}^{\infty} \left\{ x^2 \frac{1}{\sqrt{2}\Gamma(0.5)} x^{-\frac{1}{2}} e^{-\frac{x}{2}} \right\} dx - 2\nu \{E(\tilde{d}) + \nu P(\chi_1^2 > \nu)\} + \nu^2 P(\chi_1^2 > \nu) \quad (8) \\
&= \int_{\nu}^{\infty} \left\{ x^2 \frac{1}{\sqrt{2}\Gamma(0.5)} x^{-\frac{1}{2}} e^{-\frac{x}{2}} \right\} dx - 2\nu E(\tilde{d}) - \nu^2 P(\chi_1^2 > \nu) \\
&= \frac{1}{\Gamma(0.5)} \left[3\Gamma\left(0.5, \frac{\nu}{2}\right) + e^{-\frac{\nu}{2}} \sqrt{2\nu}(3 + \nu) \right] - 2\nu E(\tilde{d}) - \nu^2 P(\chi_1^2 > \nu)
\end{aligned}$$

B Consistency of the Diagnosis Method

To prove the consistency of our diagnosis model, we use the derivations in Zou (2006). To show the consistency in adaptive lasso Zou used the following conditions,

Condition B.1. *noise have independent identical distribution with mean 0 and variance σ^2*

Condition B.2. *for observation matrix X , and number of observations n , $\frac{1}{n}X^T X \rightarrow C$. Where C is a positive definite matrix.*

Condition B.1 is valid for Eq. 5. As we showed, after the transformations, the model noise has iid distribution with variance equal to 1. To show the validity of condition B.2 we need to show that this condition holds for \mathbf{A}^* instead of \mathbf{X} . We use lemma B.1 and its proof to show it.

Lemma B.1. *For \mathbf{A}^* given in Eq. 6, $\mathbf{C} = \frac{1}{p}\mathbf{A}^{*T}\mathbf{A}^*$ is a positive definite matrix*

Proof. The proof is a follows:

$$\begin{aligned}
\mathbf{A}^* &= \Lambda^{\frac{-1}{2}} \mathbf{A} \\
\mathbf{C} &= \frac{1}{p} \mathbf{A}^{*T} \mathbf{A}^* = \frac{1}{p} \mathbf{A}^T \Lambda^{\frac{-1}{2}} \Lambda^{\frac{-1}{2}} \mathbf{A} \Rightarrow \mathbf{C} = \mathbf{A}^T \Lambda^{-1} \mathbf{A}
\end{aligned}$$

To show that C is positive definite matrix it suffice to show that $x^T \mathbf{C}x > 0, \forall x \neq 0$

$$\begin{aligned} x^T \mathbf{C}x &= x^T \mathbf{A}^T \Lambda^{-1} \mathbf{A}x \\ &= z^T \Lambda^{-1} z \\ &= \sum_{i=1}^p \frac{1}{\lambda_i} z_i^2 \end{aligned}$$

Where λ_i is the pc score i. Since pc scores are positive, hence:

$$x^T \mathbf{C}x > 0, \forall x \neq 0 \quad \square$$

Since our model holds the above conditions, we can now show the consistency of our model, as follows:

Theorem B.2. *Suppose that λ in Eq. 6 varies with p . If $\frac{\lambda_p}{\sqrt{p}} \rightarrow 0$, and $\lambda_p \rightarrow \inf$, then the adaptive lasso estimate must satisfy the following:*

- *Consistency in variable selection: $\lim_p P(S^* = S) = 1$*
- *Asymptotic Normality: $\sqrt{p}(\hat{\mu}_S^* - \hat{\mu}_S) \rightarrow_d N(\mathbf{0}, \sigma')$*

Where $\sigma' = \mathbf{C}_{11}^{-1}$

Proof. for proof of Theorem, please refer to Theorem 2 in Zou (2006) □